Photoreduction of 4,4′-Bipyridine by Amines in Acetonitrile−Water Mixtures: Influence of H-Bonding on the Ion-Pair Structure and Dynamics

Olivier Poizat,* Guy Buntinx, and Laurent Boilet

Laboratoire de Spectrochimie Infrarouge et Raman (UMR 8516 de l'Université et du CNRS), Centre d'Etudes et de Recherches Lasers et Applications (FR 2416 du CNRS), Bât. C5, Université des Sciences et Technologies de Lille, 59655 Villeneuve d'Ascq, France

Received: June 24, 2005

The photoreduction of 4,4′-bipyridine (44BPY) by diazabicyclo[2.2.2]octane and triethylamine (TEA) is investigated by using picosecond transient absorption and time-resolved resonance Raman spectroscopy in various acetonitrile−water mixtures. The results are interpreted on the basis of a preferential solvation effect resulting from the presence of a specific interaction between 44BPY and water by hydrogen bonding. Below 10% water, the free 44BPY species is dominant and leads upon photoreduction to a contact ion pair that undergoes efficient intrapair proton transfer if TEA is the amine donor. Above 10% water, most of the 44BPY population is H-bonded and leads upon photoreduction to a hydrated ion pair in which the intrapair proton transfer is inhibited. Instead, the $44BPY^{-\bullet}$ species is protonated by water through the hydrogen bond with a rate constant that increases by more than 3 orders of magnitude on going from 10% to 100% water. The dependence of this rate constant on the solvent mixture composition suggests that the reaction of intracomplex proton transfer is controlled by the hydration of the residual OH^- species by three molecules of water, leading to a trihydrated $HO^-(H_2O)_3$ species.

1. Introduction

Recently, we analyzed the mechanism of photoreduction of 4,4′-bipyridine (44BPY) by aliphatic amines in acetonitrile[1] and water[2] by using picosecond transient absorption and time-resolved resonance Raman spectroscopy. In acetonitrile, it was found that the amines 1,4-diazabicyclo[2.2.2]octane (DABCO) and triethylamine (TEA) reduce the T_1 state of 44BPY to form a contact ion pair (CIP) involving the bipyridine anion radical $44BPY^{-\bullet}$ ($R^{-\bullet}$) and amine cation radical. Efficient reduction of the S_1 state also takes place but is followed by an ultrafast back electron transfer that deactivates the reaction ($\Phi^1_{deac} \sim 0.95$). The dynamics of dissociation of the triplet CIP into free ions could be followed by time-resolved Raman spectroscopy owing to slightly different vibrational frequencies of the $44BPY^{-\bullet}$ anion in the free and ion-paired forms. In the case of TEA, a fast intrapair proton-transfer reaction ($k_{PT} = 1.2 \times 10^{10}$ s^{-1}) yielding the radical 44BPYH$^\bullet$ ($RH^\bullet$) competes with the dissociation process ($k_{dis} = 2.3 \times 10^9$ s^{-1}) and quenches the ion radicals (Scheme 1).

Interestingly, the Raman spectrum of $44BPY^{-\bullet}$ was shown to be very sensitive to the presence of hydrogen bonding, providing direct information on the specific interactions of this ion with its surroundings. On this basis, it was established that in the case of photoreduction of 44BPY by TEA in acetonitrile there is no H-bonding between the ion radicals in the CIP prior to proton transfer. It was concluded that the rate of intrapair proton jump (k_{PT}) is governed by the dynamics of reorientation of the ions within the pair and occurs as soon as the mutual orientation of the ions is propitious for the transfer.

In the case of photoreduction of 44BPY by DABCO in water,[2] quenching of the S_1 state by electron transfer is essentially nonproductive, as in acetonitrile. Time-resolved Raman data revealed that the $44BPY^{-\bullet}$ species produced from the T_1 state is linked via H-bonding to solvent molecules immediately after its formation and yields rapidly the radical 44BPYH$^\bullet$ via proton transfer along the H-bond. It was tentatively suggested that the triplet ion pair produced initially in water could be solvent separated (SSIP). A reduction of the rates of diffusional quenching of the excited S_1 and T_1 states by electron transfer was observed in going from acetonitrile to water and ascribed to the increasing solvent viscosity.

In the present paper, we report an investigation of the photoreduction of 44BPY by DABCO and TEA in acetonitrile−water mixtures in order to better characterize the nature and dynamics of the triplet ion pair in the presence of water molecules in the solvent cage. Our results emphasize the determinant role of specific interaction and preferential solvation effects[3,4] on the ion pair formation and reactivity. A

SCHEME 1

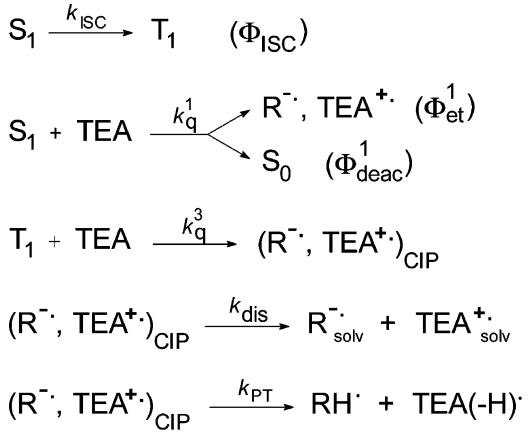

* Corresponding author. Fax: +33-320436755. E-mail: poizat@univ-lille1.fr.

10.1021/jp058199v CCC: $30.25
Published on Web 11/11/2005

particular attention has been given to the reaction of protonation of the "super" photobase $44BPY^{-\bullet}$ ($pK_a > 15$) that arises in the presence of water within a hydrogen-bonded complex, $44BPY^{-\bullet}\cdots HO-H$. This fast reaction creates a pOH jump in the solution, and our results show that the stabilization of the produced OH^- species by solvation is the rate-determining step for the proton transfer.

2. Experimental Section

4,4′-Bipyridine (44BPY), triethylamine (TEA), and 1,4-diazabicyclo[2.2.2]octane (DABCO) were purchased from Aldrich. TEA was distilled and 44BPY was sublimed at 80 °C in vacuo prior to each measurement. Acetonitrile (Prolabo, spectrophotometric grade) and DABCO were used as received. Water was distilled and deionized. Deuterium oxide (99.9 atom % D) was from Interchim. All measurements were performed on $10^{-3}-10^{-2}$ M aqueous solutions of 44BPY. Photoexcitation of 44BPY was performed within the allowed $S_0 \rightarrow S_n$ $\pi\pi^*$ transition of lowest energy (220−270 nm region) and followed by ultrafast internal conversion to a singlet S_1 $n\pi^*$ state.[5,6]

The subpicosecond transient absorption and picosecond Raman scattering setups have been already described.[5−7] Briefly, experiments were carried out by using a 1 kHz Ti−sapphire laser system based upon a Coherent (MIRA 900D) oscillator and a BM Industries (ALPHA 1000) regenerative amplifier. This system was set in a femtosecond configuration for all the absorption measurements. Tripling the initial 90 fs pulses at 800 nm (0.3 mm BBO crystal) provided the pump excitation at 266 nm. Its power was limited to 10−20 μJ per pulse (1.0−2.0 mJ/cm^2). A probe white light continuum pulse was generated at 800 nm in a CaF_2 plate. The probe pulse was delayed in time relative to the pump pulse using an optical delay line (Microcontrol Model MT160-250PP driven by an ITL09 controller, precision ±1 μm). The overall time resolution (full width at half-maximum (fwhm) of the pump−probe intensity cross-correlation) was estimated to be about 300 fs from the two-photon (pump + probe) absorption signal in pure hexane. The time dispersion of the continuum light over the 300−700 nm region of analysis was about 0.8 ps. The transmitted light was analyzed by a CCD optical multichannel analyzer (Princeton Instrument LN/CCD-1340/400-EB detector + ST-138 controller). Samples were circulating in a flow cell with 2.5 mm optical path length. Data were accumulated over 3 min (∼180000 pump−probe sequences).

For the Raman measurements, the laser source was set in a picosecond configuration. Pump pulses at 253 nm (∼15 μJ, 20 mJ/cm^2 per pulse) and probe pulses at 380 nm (∼5 μJ) were obtained by frequency tripling and doubling, respectively, the Ti−sapphire fundamental tuned at 760 nm. The pump−probe cross correlation fwhm was ∼4 ps. Scattered light was collected at 90° to the incident excitation and sent through a Notch filter into a home-built multichannel spectrometer coupled to a CCD optical multichannel analyzer (Princeton Instrument LN/CCD-1100-PB−UV/AR detector + ST-138 controller). The flowing jet sampling technique was adopted (1 mm diameter jet). The wavenumber shift was calibrated using the Raman spectra of indene. Data collection times were 10−20 min. In all absorption and Raman measurements, the pump−probe polarization configuration was set at the magic angle.

3. Results

A. Preferential Solvation Effects in Acetonitrile−Water Mixtures. The Raman spectrum of 44BPY in the ground state is very sensitive to the formation of hydrogen bonds at the nitrogen atoms.[1,2] Four Raman-active modes were found to be significantly shifted to higher frequencies on going from aprotic to protic solvents.[2] We have analyzed this effect in more detail in acetonitrile−water mixtures. Figure 1 presents the dependence of the Raman frequency of the most sensitive vibration, the symmetric ring breathing mode, on the water content (in volume). The variation is highly nonlinear and shows two distinct solvation regimes. From 0% to 10% water, the frequency increases rapidly from 997 to 1005 cm^{-1}. This shift is attributable to the formation of hydrogen bonding[2] and denotes a phenomenon of preferential solvation[3,4] of 44BPY by water. The solute−solvent interaction is thus dominated by specific solvent hydrogen bond acidity interactions. Then, from 10% to 100% water, the frequency value shifts much more slowly from 1005 to 1009.5 cm^{-1}, which is probably the consequence of a gradual increase of nonspecific solute−solvent interactions. Enhancing the water content from 10% to 100% increases the number of water molecules in the solvent shell of the H-bonded 44BPY−water species, which causes an increase of the local polarity due to the higher dielectric constant (ϵ) and Kamlet−Taft polarity (π^*) of water relative to acetonitrile. According to Reichardt,[8,9] the solvent polarity can be defined as the overall solvation capability of solvents, involving specific as well as nonspecific interactions with the solutes. In this regard, the 44BPY vibrational frequency analyzed above (Figure 1) appears to be a good probe for evaluating the polarity of solvent mixtures as it is sensitive to both the specific and nonspecific solute−solvent interactions. As a confirmation, the behavior observed in Figure 1 for the 44BPY frequency is very similar to that reported[4] for the Dimroth−Reichardt polarity parameter, E_T, calculated from the peak position of the absorption spectrum of the solvatochromic indicator betaine in binary mixtures of protic and aprotic solvents and fitted by a preferential solvation model[10] based on solvent-exchange equilibria. Comparable results were found for the solvatochromic probe coumarin 153[11,12] and 102 dyes.[12] Note that from experimental[13−18] and theoretical[19−22] studies of the structural properties of the acetonitrile−water mixtures it is generally predicted that the binary solution contains structural microheterogeneities in the solvent composition, with water-rich and acetonitrile-rich clusters:[13,14,17−20,23] acetonitrile molecules aggregate with dipole−dipole interaction of CN groups and water molecules aggregate with hydrogen bonding. In this assumption, the preferential solvation effect observed above would indicate that 44BPY becomes predominantly confined in water-rich microdomains as soon as the water content reaches 10%.

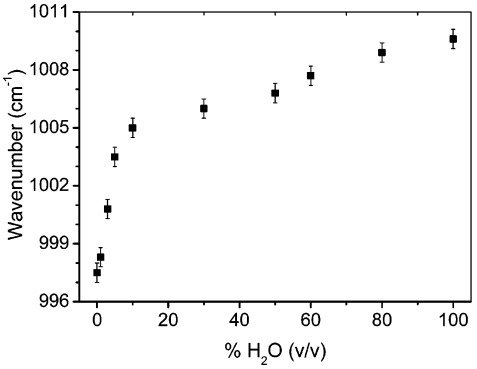

Figure 1. Variation of the Raman frequency of the S_0 44BPY symmetric ring breathing mode as a function of the water content (in volume) in acetonitrile−water solvent mixtures.

Similar frequency dependence on the solvent composition in acetonitrile−water binary mixtures was observed for some solvent-sensitive Raman modes of DABCO and TEA (not

shown) and revealed that preferential solvation of these amines by water is also achieved for water content ≥10−15%.

B. Photoreduction of 44BPY by DABCO. Transient absorption spectra of solutions of 44BPY and DABCO in acetonitrile-water mixtures were recorded as a function of the water content and for four DABCO concentrations (0.1−0.8 M range), at different pump−probe time delays in the 0−1500 ps domain. The 266-nm pump wavelength matches the lowest energy $\pi\pi^*$ absorption band of 44BPY ($\epsilon_{266} = 7500\ M^{-1}\ cm^{-1}$). The absorption of DABCO at 266 nm is very weak, but efficient photoionization can take place at the high concentrations used in our study. To avoid this undesirable reaction, the concentration in 44BPY was raised to 10^{-2} M, in which case the excitation of DABCO was found to be negligible.[2]

Before 100 ps, the data show, as in pure acetonitrile or in pure water, the decay of the S_1 state spectrum ($\lambda_{max} = 381 \pm 1$ and 585 ± 5 nm) and the appearance of the T_1 state spectrum ($\lambda_{max} = 335 \pm 5$ nm). The formation of photoreduction products is not detected although the S_1 state is strongly quenched by DABCO, which is in agreement with previous observations that the intrapair back electron transfer is ultrafast within the singlet ion pair.[1,2] Examples of spectral evolution in the 100−1500 ps time range are shown in Figure 2 for solutions of 44BPY (10^{-2} M) and DABCO (0.5 M) in mixtures of acetonitrile and 5% (part A), 26% (part B), and 40% (part C) water by volume. In all cases we observe the decay of the triplet-state band at 335 nm and the appearance of two sets of additional absorption signals with distinct kinetic behaviors. One, characterized by a sharp peak at 380 nm and a broad band covering the 500−650 nm region with three rough maxima, corresponds to the anion radical spectrum[24] produced upon diffusional reduction of the T_1 state by DABCO. The second one, presenting two bands in the 360−369 nm and 525−542 nm domains, respectively, is ascribable to the N-hydro radical, 44BPYH$^{\bullet}$,[25−27] produced by protonation of the 44BPY$^{-\bullet}$ anion radical by water. Whereas this spectrum increases continuously with time, the 44BPY$^{-\bullet}$ spectrum increases at short time and then decreases. In the decay region, isosbestic points are noticed at 373 (see right inset in Figure 2, parts B and C) and 570 nm between the anion and radical spectra. The anion decay and radical appearance are extremely slow at low water content (at 5% water (part A), they are even not perceptible in the 0−1500 ps time domain) but accelerate drastically upon increasing the amount of water. Note that the weak and broad absorption band of DABCO$^{+\bullet}$, expected in the 350−650 nm domain (ϵ_{max} 2100 $M^{-1}\ cm^{-1}$), is not clearly detected, probably because it is obscured by the much more intense 44BPY$^{-\bullet}$ spectrum.

Before going into the detail of the reaction mechanism, it is worth examining the band position of the anion absorption spectrum. A notable shift of the vibronic maxima of the 44BPY$^{-\bullet}$ visible band has been reported to occur on changing the solvent from acetonitrile (555, 580, and 638 nm) to water (530, 562, and 604 nm) and ascribed to the formation of H-bonding in water.[2] We have monitored more precisely the spectral evolution as a function of the solvent composition in the acetonitrile−water mixtures. Figure 3 shows a plot of the peak position of the lowest energy component as a function of the water content. The variation is highly nonlinear, with an abrupt shift upon increasing the water content in the acetonitrile-rich region followed by a weaker shift in the 10−100% water domain. This evolution parallels that observed for the establishment of hydrogen bonding in the ground state (Figure 1); i.e., the same effect of preferential solvation by water is observed for both the neutral and anionic species. This correlation

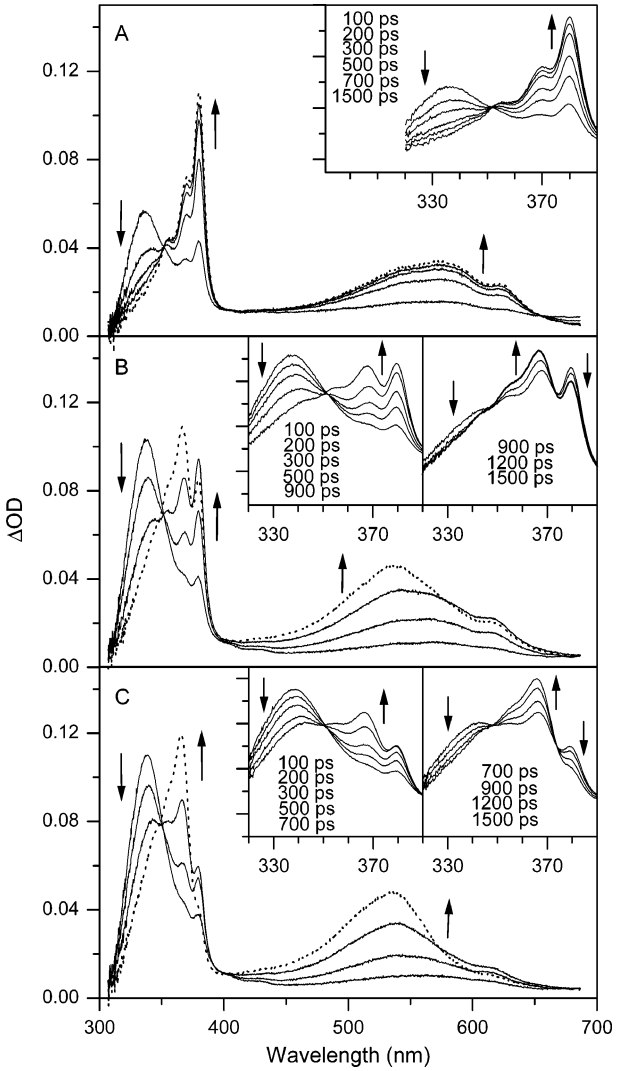

Figure 2. Transient absorption spectra of solutions of 44BPY (10^{-2} M) and DABCO (0.5 M) in mixtures of acetonitrile and (A) 5%, (B) 26%, and (C) 40% water by volume, at four delay times (100, 300, 700, and 1500 ps) after 266 nm excitation. Vertical arrows indicate the signal evolution. The insets show enlargements of the 320−390 nm region for various spectra in the 100−1500 ps time domain (delay times are indicated).

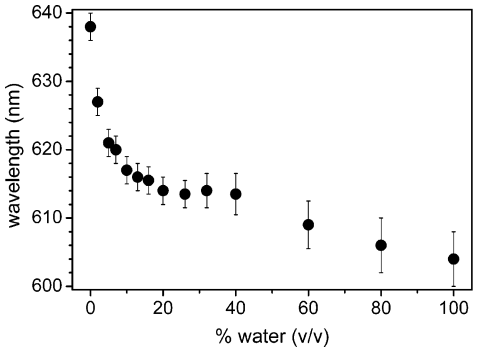

Figure 3. Variation of the peak position of the lowest energy vibronic component in the transient absorption spectrum of the 44BPY$^{-\bullet}$ anion radical as a function of the water content in acetonitrile−water solvent mixtures.

indicates that when 44BPY is H-bonded to a water molecule before excitation, the anion produced by photoreduction is also H-bonded. The H-bonded water molecule remains thus attached to—or in the vicinity of—the heterocyclic molecule through the successive photophysical steps from S_0 to R$^{-\bullet}$.

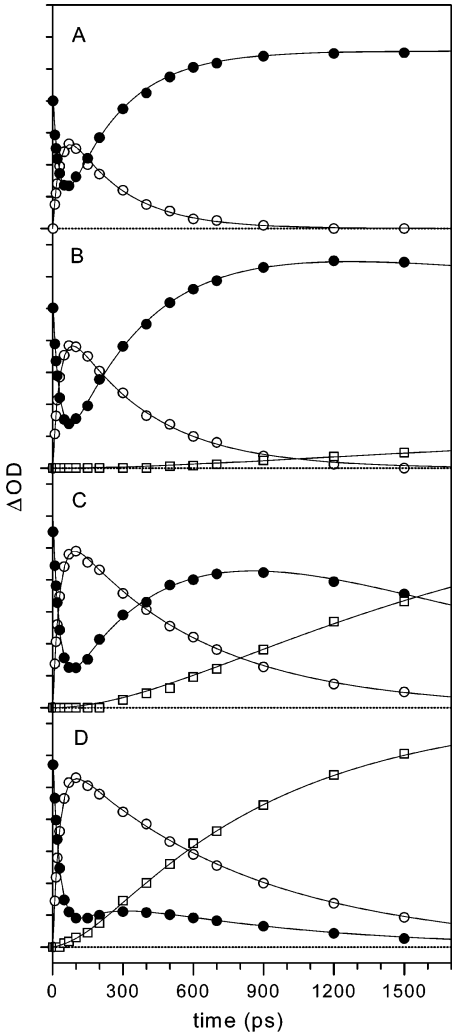

Figure 4. Time dependence of the extracted contributions of the T_1 state absorption at 339 nm (○), N-hydro radical absorption at 365 nm (□), and residual absorption (S_1 state + anion radical) at 381 nm (●) and the best fit (solid lines) based on reaction Scheme 2 (see the text) for solutions of 44BPY (10^{-2} M) and DABCO (0.5 M) in mixtures of acetonitrile and (A) 5%, (B)13%, (C) 26%, and (D) 60% water by volume following excitation at 266 nm. In all cases the ΔOD increment is 0.02 and the dashed line corresponds to ΔOD = 0.

To examine quantitatively the reaction mechanism, the time evolution of the transient absorption spectra has been analyzed into three contributions as described previously.[2] The results are shown in Figure 4 for solvent mixtures of 5, 13, 26, and 60% water in volume and a DABCO concentration of 0.5 M. A first contribution (symbol ○) corresponds to the T_1 state signal at 339 nm, a second one (symbol □) to the 44BPYH• radical signal at 365 nm, and the last contribution (symbol ●) to the sum of the S_1 state and $44BPY^{-\bullet}$ anion signals at 381 nm (these two species have similar and overlapping spectra). The extinction of the S_1 state population is responsible for the fast decay observed at short time on this latter component. These kinetic data were fitted according to the sequential electron transfer−proton transfer reaction model found in neat water,[2] in which the reduction of the 44BPY T_1 state by DABCO is followed by the protonation of the resulting $44BPY^{-\bullet}$ anion by the surrounding water to yield the N-hydro radical (Scheme 2).

Although the S_1 state quenching process was considered as almost nonproductive ($\Phi^1_{et} \ll \Phi^1_{deac}$), it was included in the fitting reaction model to account for the variation of the T_1 state yield (Φ_{ISC}) with the DABCO concentration and water content

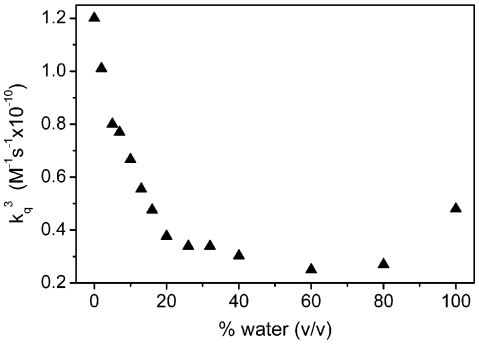

Figure 5. Variation of the rate constant k^3_q of quenching of the 44BPY triplet state by DABCO as a function of the water content in acetonitrile−water solvent mixtures.

SCHEME 2

$$S_1 \xrightarrow{k_{ISC}} T_1 \quad (\Phi_{ISC})$$

$$S_1 \xrightarrow[DABCO]{k^1_q} R^{-\cdot} \quad (\Phi^1_{et})$$

$$\qquad\qquad\quad \rightarrow S_0 \quad (\Phi^1_{deac})$$

$$T_1 \xrightarrow[DABCO]{k^3_q} R^{-\cdot} \quad (\Phi^3_{et})$$

$$R^{-\cdot} \xrightarrow[H_2O]{k_H} RH^{\cdot}$$

in the solution. The yields of dissociation of the singlet ion pair into free ions (Φ^1_{et}) and of deactivation of the S_1 state by intrapair charge recombination (Φ^1_{deac}) were fixed to the same ratio 0.05:0.95 as in neat water.[2] The singlet and triplet state quenching rate constants k^1_q and k^3_q and the anion protonation rate constant k_H were set as variable parameters. The analysis was made in the hypothesis of diffusional electron-transfer quenching (static electron-transfer quenching was found negligible for [DABCO] < 1 M[2]). The singlet and triplet state decay rate constants were thus assumed to obey the pseudo-first-order kinetics $k^1 = k_{ISC} + k^1_q[DABCO]$ and $k^3 = (\tau^3_0)^{-1} + k^3_q[DABCO]$, respectively, where τ^3_0 is the T_1 state lifetime in the absence of DABCO (~70 μs[28]). This hypothesis was confirmed by the fact that, for each acetonitrile−water mixture, nearly the same set of k^1_q and k^3_q values was found for the different DABCO concentrations experienced. On the other hand, the $44BPY^{-\bullet}$ decay and 44BPYH• growth were well fitted by single-exponential kinetics (rate constant k_H), which denotes a first-order or pseudo-first-order proton-transfer process. Excellent agreement between the experimental and calculated kinetics concerning the profiles as well as the relative amplitudes was obtained in all cases.

Both the k^3_q and k_H rate constants appear to be significantly sensitive to the solvent mixture composition. Figure 5 shows a plot of k^3_q as a function of the water amount in the solution. It presents a fast decrease in the acetonitrile-rich region and a slight increase in the water-rich region. On the other hand, the $44BPY^{-\bullet}$ protonation rate k_H increases by more than 3 orders of magnitude on going from 10% water in acetonitrile ($k_H = 4.0 \times 10^7\ s^{-1} \ll k_{PT}$) to pure water ($k_H = 7.7 \times 10^{10}\ s^{-1} > k_{PT}$). Plotting the rate constant k_H versus the water concentration on a double-logarithmic scale (Figure 6) shows a linear dependence with a slope of 3.1 ± 0.2. It reveals that roughly

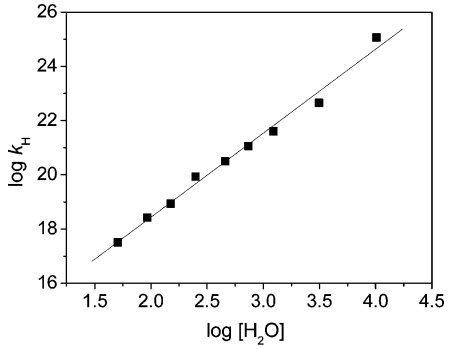

Figure 6. Dependence of the rate constant k_H (in s^{-1}) of protonation by water of the 44BPY$^{-\bullet}$ anion radical on water concentration (in M) in acetonitrile−water solvent mixtures (DABCO concentration of 0.5 M).

three water molecules are involved in the proton-transfer reaction, according to eq 1

$$k_H = k_h[H_2O]^3 \quad (1)$$

where k_h is a rate constant of quenching of 44BPY$^{-\bullet}$ by proton transfer. Finally, it is interesting to examine the influence of DABCO on the k_H value. In pure water, it has been observed that k_H was lowered from 7.7×10^{10} to 2.5×10^{10} s^{-1} on going from 0.5 to 1.6 M DABCO[2]. Figure 7 presents the time evolution of the extracted T_1 state, 44BPYH$^\bullet$ radical, and (S_1 state + 44BPY$^{-\bullet}$ anion) contributions obtained in an acetonitrile (80%)/water (20%) solvent mixture for various DABCO concentrations. The best fits to the data using reaction Scheme 2 are also shown. The increase of the quenching rate constants k^1_q and k^3_q with the DABCO content is manifested in Figure 7 by the reduction of the T_1 state yield (maximal amplitude of the T_1 state kinetics) and decay time, respectively, on going from A to D. On the other hand, the increase of the ratio of the anion to radical amplitudes at 1500 ps on going from B to D is indicative of a reduction of the rate of protonation of the anion upon increasing the amine content. This conclusion is confirmed by the plot of k_H as a function of the DABCO concentration displayed in Figure 8. The same effect is observed at all acetonitrile−water solvent compositions.

Pump−probe time-resolved resonance Raman measurements were also performed on solutions of 44BPY and DABCO in the same acetonitrile−water mixtures as those studied by transient absorption. According to the UV−visible absorption characteristics of the different transient species involved in the photoreduction of 44BPY, the 380-nm probe excitation wavelength employed in these measurements is in good resonance conditions for the S_1 state, anion radical and N-hydro radical, but almost out of resonance for the T_1 state. The spectral evolution shows, as previously reported in neat water,[2] the fast decay of the S_1 state Raman bands below 100 ps and the appearance of the anion and radical spectra in the 100−1500 ps time range. The kinetics are consistent with those obtained by transient absorption. As for the 44BPY ground state, several Raman frequencies of 44BPY$^{-\bullet}$ are very sensitive to the formation of hydrogen bonding with solvent molecules[1,2,28] and allow probing the state of solvation of the ion. Among them, the highest energy phenyl-type ring deformation mode in the 1600 cm^{-1} region (Wilson mode 8a[29]) is the only one that is well distinguishable from the Raman-active vibrations of the 44BPYH$^\cdot$ radical (see Figure 5 in ref 2) also present in the spectra. We have thus plotted the 44BPY$^{-\bullet}$ 8a frequency, measured at a pump−probe delay of 500 ps, as a function of

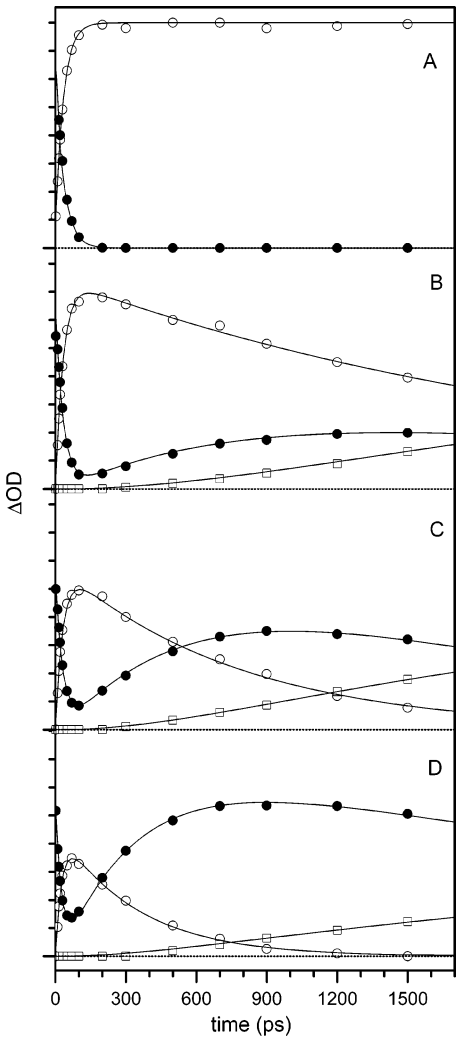

Figure 7. Time dependence of the extracted contributions of the T_1 state absorption at 339 nm (○), N-hydro radical absorption at 365 nm (□), and residual absorption (S_1 state + anion radical) at 381 nm (●) and the best fit (solid lines) based on reaction Scheme 2 (see the text) for acetonitrile (80%)−water (20%) solutions of (A) 44BPY (10^{-2} M), (B) 44BPY (10^{-2} M) and DABCO (0.1 M), (C) 44BPY (10^{-2} M) and DABCO (0.3 M), and (D) 44BPY (10^{-2} M) and DABCO (0.8 M) following excitation at 266 nm. In all cases the ΔOD increment is 0.02 and the dashed line corresponds to ΔOD = 0.

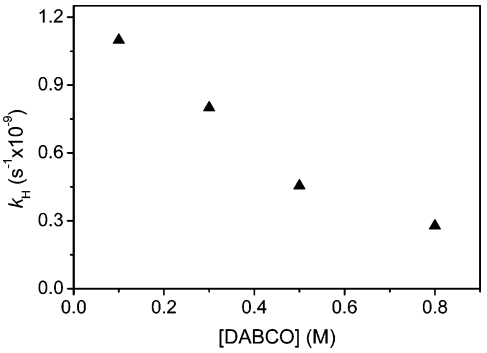

Figure 8. Variation of the rate constant k_H of protonation of the 44BPY$^{-\bullet}$ anion radical by water in an acetonitrile (80%)−water (20%) solution as a function of the DABCO concentration.

the water content (Figure 9). From 0 to 10% water, the 8a frequency increases abruptly from its value in pure acetonitrile (1605 cm^{-1}) to the value observed in pure water (1611 cm^{-1}). Above 10% water, the frequency remains unchanged. This behavior is comparable to that observed above (Figure 3) for

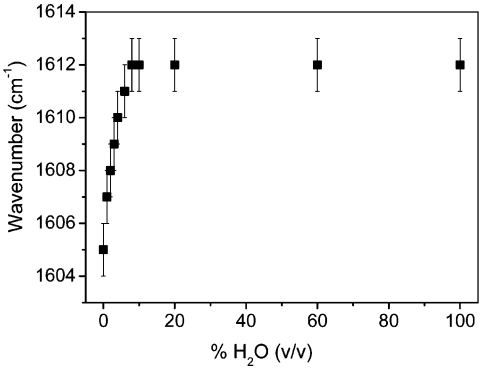

Figure 9. Variation of the 44BPY$^{-\bullet}$ frequency of the Raman active phenyl-type ring deformation vibrational mode 8a, probed at a delay time of 500 ps after 266 nm excitation, as a function of the water content in acetonitrile−water solvent mixtures.

the position of the visible absorption band of 44BPY$^{-\bullet}$. It confirms definitely the assumption of preferential solvation of the anion by water due to hydrogen bonding. Consider now the time dependence of the 8a frequency. At low water content (<10%), the frequency value drifts with time from 1601 ± 1 cm^{-1} at 10 ps to 1605 ± 1 cm^{-1} at 1500 ps. This time-dependent shift is analogous to that measured previously in neat acetonitrile and ascribed to the dissociation of the CIP into free ions.[1] In contrast, as in pure water,[2] no shift is observed in the 0−1500 ps domain for water content ≥10% and mode 8a keeps a frequency value of 1611 cm^{-1} at all times. We shall address these observations in more detail in section C in light of the results obtained about the photoreduction by the amine TEA.

C. Photoreduction of 44BPY by TEA. Transient absorption spectra of solutions of 44BPY and TEA in acetonitrile−water mixtures were recorded as a function of the water content and for four TEA concentrations (0.2−0.9 M range), at different pump−probe time delays in the 0−1500 ps domain. Figure 10 shows spectra obtained for solutions of 44BPY (10^{-2} M) and TEA (0.4 M) in acetonitrile (part A) and in mixtures of acetonitrile and 1% (part B), 5% (part C), and 30% (part D) water by volume. As in the case of DABCO, these spectra are characteristic of the T_1 state (∼330-nm band) and of the reduction products, 44BPY$^{-\bullet}$ (378-nm and 500−650-nm bands) and 44BPYH$^{\bullet}$ (∼360-nm and 530-nm bands). It can be seen in Figure 10 that the ratio of these two products and their dynamics depend strongly on the water content. The 100-ps spectrum is about the same in all cases (parts A−D) and is characterized, besides the strong T_1-state band, by a predominant contribution of the anion spectrum over the radical spectrum. Beyond 100 ps, the spectral evolution in pure acetonitrile (part A) shows essentially the decay of T_1 and the growth of the radical species that becomes the major product at 1500 ps. This evolution has been explained[1] by the fact that the dissociation of the CIP formed initially from reduction of the T_1 state is 5 times slower than the intrapair proton transfer (see Scheme 1). Upon addition of up to 10% water in volume, the relative amplitudes of the anion and radical spectral rises are progressively inversed. At 5% water (Figure 10, part C), the rise of the anion spectrum is already dominant. It seems that the fast intrapair proton transfer observed in pure acetonitrile does not occur or is strongly attenuated in the presence of water. At higher percentage of water (example: part D, 30% water), the ratio of the final products changes again in favor of the radical since the anion stops rising rapidly, and then decays, whereas the radical species grows continuously. In pure water (not shown), the anion species is entirely replaced by the radical within 800 ps. The behavior observed for solutions of 10−100% water appears thus comparable to that found above in the case of DABCO and is likely characterizing the protonation of the anion by water. As expected, the absorption maximum of the 44BPY$^{-\bullet}$ UV band shows the same dependence on the solvent composition as that displayed in Figure 3, typical of the preferential solvation phenomenon.

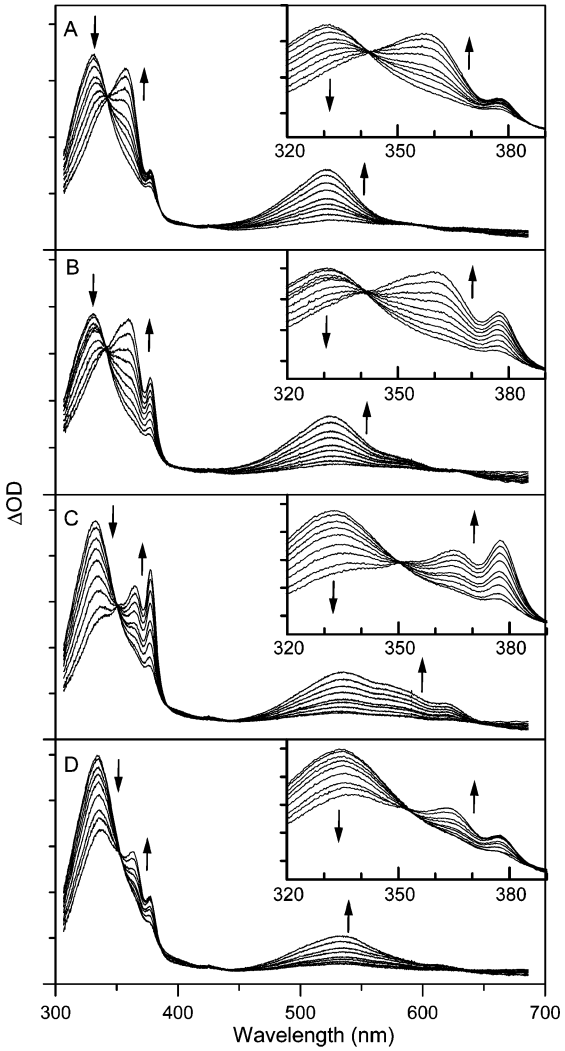

Figure 10. Transient absorption spectra of solutions of 44BPY (10^{-2} M) and TEA (0.4 M) in (A) neat acetonitrile and in mixtures of acetonitrile and (B) 1%, (C) 5%, and (D) 30% water by volume, at nine delay times (100, 200, 300, 400, 500, 700, 900, 1200, and 1500 ps) after 266 nm excitation. The ΔOD increment is 0.02 in all cases. Vertical arrows indicate the signal evolution. The insets show enlargements of the 320−390 nm region.

The time evolution of the transient absorption spectra was analyzed into the T_1 state, anion, and radical contributions as described in section B and fitted according to the procedure defined below. Figure 11 presents the results obtained in a solvent mixture of 5% water in acetonitrile (part B) compared to those in pure acetonitrile (part A), for a TEA concentration of 0.6 M. In pure acetonitrile, the experimental data were fitted according to the reaction Scheme 1 as previously.[1] In pure water, the data could be fitted using the two-step reaction Scheme 2 employed above for the photoreduction of 44BPY by DABCO in water, confirming that the formation of the radical results purely from the protonation of the anion by water. This fast protonation reaction ($k_H = 6 \times 10^{10}$ s^{-1} for a TEA concentration of 0.6 M) quenches notably the intrapair proton transfer ($k_{PT} = 1.2 \times 10^{10}$ s^{-1}) and ion pair dissociation ($k_{dis} = 2.3 \times 10^{9}$ s^{-1}) processes observed in acetonitrile (Scheme 1) in such a way

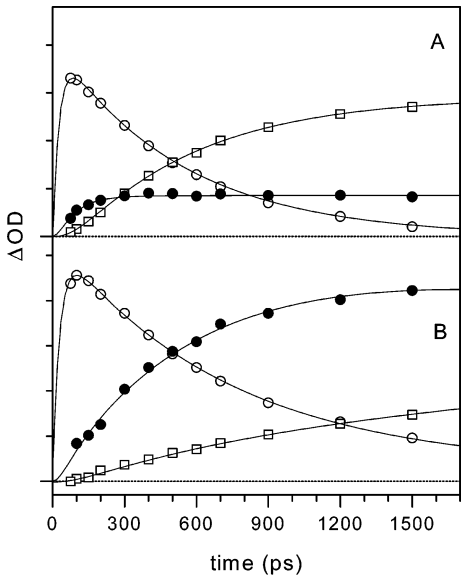

Figure 11. Time dependence of the extracted contributions of the T_1 state absorption at 339 nm (○), N-hydro radical absorption at 365 nm (□), and residual absorption (S_1 state + anion radical) at 381 nm (●) and the best fit (solid lines) based on reaction Scheme 4 (see the text) for solutions of 44BPY (10^{-2} M) and TEA (0.6 M) in (A) neat acetonitrile and in (B) acetonitrile containing 5% water by volume following excitation at 266 nm. In all cases the ΔOD increment is 0.02 and the dashed line corresponds to ΔOD = 0.

that no information on the ion pair reactivity can be obtained in pure water. In solutions containing 10−100% water in volume, the experimental kinetics can still be fitted using the two-step reaction Scheme 2. The overall reaction scheme is thus typical of that in pure water; i.e., no intrapair proton transfer occurs. As in the case of the reduction by DABCO, the anion formed from the reduction by TEA is protonated by water with a rate significantly decreasing with the decrease of the amount of water in the solution. The dependence of the protonation rate constant k_H is similar to that displayed in Figure 6. At 10% water, k_H is much lower ($\sim 2 \times 10^8$ s^{-1}) than the intrapair proton-transfer rate constant k_{PT} measured in acetonitrile. The lack of intrapair proton transfer from $TEA^{+\bullet}$ to $44BPY^{-\bullet}$ can thus no longer be simply attributed to the quenching by water. It must be assumed that the k_{PT} value itself is drastically lowered in the presence of water. Finally, in acetonitrile-rich solutions, the experimental kinetics show a rapid switch from the "pure acetonitrile regime" to the "pure water regime" on going from 0 to 10% water. In a first attempt to fit these data, we considered that a CIP is produced upon photoreduction in all acetonitrile−water mixtures, having the same intrapair reactivity (k_{PT}) as in pure acetonitrile, regardless of whether the anion is H-bonded to water or not within the ion pair. Accordingly, a reaction model based in Scheme 1 and complemented by an additional step of protonation of the solvated anion by water (Scheme 3) was tested.

This model failed resolutely to account for the experimental data. Indeed, it appeared impossible to fit simultaneously the anion and radical time evolutions. For example, fitting properly the T_1 state and anion evolutions in Figure 11, part B (5% water), required to reduce notably the intrapair proton-transfer rate (k_{PT}) compared to the value in pure acetonitrile and led to a calculated radical kinetics showing much slower rise at short time and much smaller final amplitude than observed. The only way to get a good fit of the profiles and relative amplitudes of the experimental T_1 state, anion, and radical evolutions for all the experienced solvent mixtures was to consider the presence

SCHEME 3

$$S_1 \xrightarrow{k_{ISC}} T_1 \quad (\Phi_{ISC})$$

$$S_1 + TEA \xrightarrow{k_q^1} R^{-\bullet}, TEA^{+\bullet} \quad (\Phi_{et}^1)$$
$$\qquad\qquad\quad\; S_0 \quad (\Phi_{deac}^1)$$

$$T_1 + TEA \xrightarrow{k_q^3} (R^{-\bullet}, TEA^{+\bullet})_{CIP}$$

$$(R^{-\bullet}, TEA^{+\bullet})_{CIP} \xrightarrow{k_{dis}} R^{-\bullet}_{solv} + TEA^{+\bullet}_{solv}$$

$$(R^{-\bullet}, TEA^{+\bullet})_{CIP} \xrightarrow{k_{PT}} RH^{\bullet} + TEA(-H)^{\bullet}$$

$$R^{-\bullet}_{solv} \xrightarrow[H_2O]{k_H} RH^{\bullet}$$

of two types of triplet ion pairs of concentration ratio depending on the water content. One is the CIP produced in pure acetonitrile with a reactivity characterized by Scheme 3 (intrapair proton transfer, ion pair dissociation, and slow pseudo-first-order protonation of the free anion by water). The contribution of this CIP to the overall ion pair population appears to decrease upon increasing the amount of water in the solution and becomes insignificant above 10% water. The rate constants for ion pair dissociation, k_{dis}, and intrapair proton transfer, k_{PT}, keep approximately the same values as in pure acetonitrile. The second ion pair differs from the CIP by the fact that it does not undergo intrapair proton transfer. All the same, the $44BPY^{-\bullet}$ species involved in this pair yields the N-hydro radical by protonation by water (rate k_H) as well as the solvated anion arising from dissociation of the pair. Absent in pure acetonitrile, the contribution of this second type of ion pair increases with the water content until 10% water whereas the CIP contribution vanishes. Above 10% water, only the second type of ion pair is present. At 5% water (Figure 11, part B), the ratio of its concentration to the CIP concentration is 3:1. From evidence, the variation of the relative populations of the two ion pairs as a function of the solvent composition matches the spectral changes (Figures 3 and 9) that characterize the phenomenon of preferential solvation of $44BPY^{-\bullet}$ by water discussed above. It can be concluded that the ion pair predominantly produced in the presence of water involves an H-bonded $44BPY^{-\bullet}$ species. This "hydrated" ion pair is named "HIP". Since the preferential solvation effects characterizing the neutral (ground state) and anionic forms of 44BPY are correlated, the concentration ratio of the HIP and CIP produced on photoreduction at a given solvent composition is likely determined by the ratio of the initial free and H-bonded 44BPY populations in the solution. The triplet state reaction mechanism related to the HIP is recapitulated in Scheme 4. In this scheme, the excited singlet and triplet states are expressed as (S_1, H_2O) and (T_1, H_2O) to indicate that the water molecule that is H-bonded to 44BPY in the ground state remains attached to (or in the vicinity of) the excited species until the reduction process.

The spectral evolution obtained from time-resolved resonance Raman measurements of solutions of 44BPY and TEA in acetonitrile−water mixtures is in agreement with the absorption results. The spectra recorded in pure acetonitrile, already published,[1] show the rise of the anion and that, delayed in time, of the radical resulting from the intrapair proton transfer. As in the case of DABCO, the frequency of the solvent-sensitive phenyl-ring mode 8a of the anion is characteristic of the absence

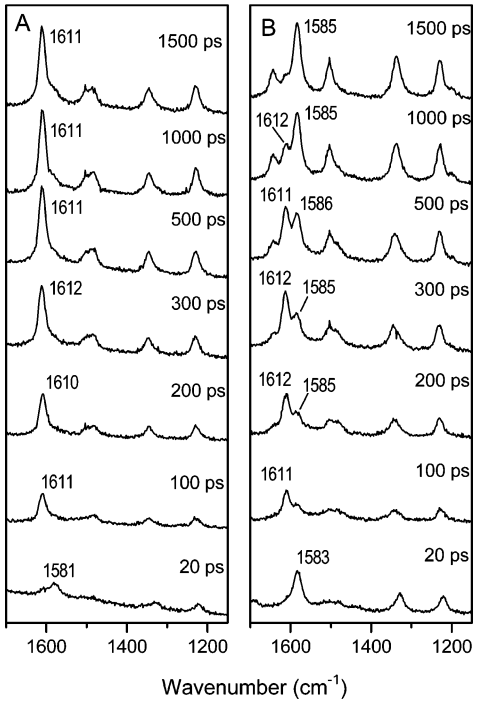

Figure 12. Time-resolved resonance Raman spectra of solutions of 44BPY (10^{-3} M) and TEA (0.6 M) in solutions of (A) 10% and (B) 30% water in acetonitrile probed at 380 nm at different delay times (20−1500 ps) after pump excitation at 253 nm. The probe-only spectrum (solvent and ground-state peaks) has been subtracted to all spectra. Some characteristic Raman frequencies are indicated.

SCHEME 4

$$(S_1, H_2O) \xrightarrow{k_{ISC}} (T_1, H_2O)$$

$$(T_1, H_2O) + TEA \xrightarrow{k_q'^3} (R^{-\cdot}...HO\text{-}H, TEA^{+\cdot})_{HIP}$$

$$(R^{-\cdot}...HO\text{-}H, TEA^{+\cdot})_{HIP} \xrightarrow{k'_{dis}} (R^{-\cdot}...HO\text{-}H)_{solv} + TEA^{+\cdot}_{solv}$$

$$(R^{-\cdot}...HO\text{-}H, TEA^{+\cdot})_{HIP} \xrightarrow{k_H} RH^{\cdot} + OH^{-} + TEA^{+\cdot}$$

$$(R^{-\cdot}...HO\text{-}H)_{solv} \xrightarrow{k_H} RH^{\cdot} + OH^{-}$$

of H-bonding and increases with time from 1600 to 1605 cm^{-1}. This shift, ascribed to the passage of the ion-paired anion to the free anion,[1] arises concomitantly with the growth of the radical spectrum, as expected from the fact that the appearance of the free anion and of the radical are characterized by the same rate constant ($k_{PT} + k_{dis}$) as the ion-pair decay kinetics. In solvent mixtures containing 10−100% water in volume (examples of Raman data for 10% and 30% water are shown in Figure 12, A and B, respectively), the $44BPY^{-\bullet}$ 8a mode appears at 1611 ± 1 cm^{-1}, a value typical of the H-bonded anion. As observed by transient absorption, the rate of appearance of the $44BPYH^{\bullet}$ radical spectrum due to protonation of the anion is much slower than in pure acetonitrile and increases with the amount of water in the solution. At 10% water (Figure 12, part A), the rate is so slow that the typical radical band at 1585 cm^{-1} is seen as a weak shoulder on the side of the 1611 cm^{-1} band of the anion. At 30% water (Figure 12, part B), the rise of the 1585 cm^{-1} peak and decay of the 1611 cm^{-1} band are clearly faster. These results confirm that the intrapair proton transfer does not occur above 10% water, in agreement with the reaction Scheme 4. As found in the case of DABCO, the 1611 cm^{-1} anion frequency does not evolve with time. The dissociation of the HIP is thus not characterized spectrally (k'_{dis} remains unknown), in such a way that the measured rate constant value k_H may correspond either to the protonation of the anion within the HIP or to the protonation of the dissociated anion, $(R^{-\bullet}\cdots HO-H)_{solv}$, or both.

4. Discussion

The results presented above concerning the T_1 state reduction process of 44BPY by TEA in acetonitrile−water mixtures can be summarized as follows. In neat acetonitrile, a CIP (contact ion pair) is formed and the reaction scheme is reduced to Scheme 1. In acetonitrile−water mixtures with water ≥10% in volume, a HIP (hydrated ion pair) is produced, in which the 44BPY anion is H-bonded to water, and the reaction is described by Scheme 4. In the 0−10% water concentration domain, both the CIP and HIP are present, with reactivities characterized by Schemes 3 and 4, respectively. Their relative concentrations are proportional to the initial free and H-bonded ground state 44BPY populations, respectively, determined themselves by the preferential solvation effect. These two ion pairs can be distinguished experimentally from each other owing to their different reactivity. In fact, the CIP undergoes efficient intrapair proton transfer ($\Phi_{RH^{\bullet}} = k_{PT}/(k_{PT} + k_{dis}) \sim 0.84$) but the HIP does not. The CIP dynamics is characterized by the rate k_{PT} of appearance of the $44BPYH^{\bullet}$ radical via this intrapair reaction as well as by the time dependence of the frequency of the anion vibration 8a, sensitive to the passage from the ion paired anion to the free anion. In contrast, no information is available on the HIP dynamics since, on one hand, it is not distinguishable spectrally from the solvated ions, $(R^{-\bullet}\cdots HO-H)_{solv}$, and, on the other hand, does not manifest any specific reactivity. Whereas at low water content (10−30%) the protonation of the H-bonded $44BPY^{-\bullet}$ anion by water is so slow that it certainly occurs after the dissociation of the pair, in pure water it probably takes place within the HIP. The fact that there is no discontinuity in the variation of the protonation rate k_H with the solvent mixture composition from 10 to 100% water (Figure 6) indicates that the HIP dynamics cannot be determined by this way either.

Similar preferential solvation properties are observed for $44BPY^{-\bullet}$ in the case of reduction by DABCO and TEA. The formation of CIP and HIP pairs with concentration ratios equally dependent on the solvent mixture composition is thus likely taking place in both cases. However, in the case of DABCO, it is not possible to distinguish experimentally these two types of ion pairs as in the case of TEA because the CIP does not undergo intrapair proton transfer (the cation of DABCO is much less acidic than the TEA one[30]). Accordingly, it can be assumed that the photoreduction of 44BPY by DABCO in acetonitrile−water mixtures follows a reaction scheme equivalent to a combination of Scheme 3 (in which the intrapair proton-transfer process, k_{PT}, must be omitted) and Scheme 4.

The inhibition of the intrapair proton transfer from $TEA^{+\bullet}$ in the presence of ≥10% water is related to the change of the ion-pair structure and/or dynamics on going from the CIP to the HIP. A possible explanation is that H-bonding between water and 44BPY prevents any close contact of the two reaction partners before as well as after the transfer of electron; i.e., the HIP would be equivalent to a solvent separated ion pair (SSIP). This hypothesis is consistent with the fact that the ion pair could not be characterized spectrally. Indeed quite similar environments are expected for ions involved in SSIP and solvated ions. In this assumption, the initial electron transfer from TEA to the excited 44BPY species occurs through a solvent layer but the intrapair proton-transfer process is inhibited, in agreement

with the fact that the barrier for proton transfer is known to increase much faster than the barrier for electron transfer upon increasing the distance between the donor and acceptor partners.[31−34] However there is no real experimental evidence for the formation of a SSIP. An alternative hypothesis is that a CIP is formed in all cases but, in the presence of water, the proton accepting site on $44BPY^{-\bullet}$ is not available for intrapair transfer because it is involved in the H-bonding with water. In contrast to the situation found in pure acetonitrile (see the introduction), the dynamics of reorientation of the ions within the pair cannot allow finding a conformation where the mutual ion orientation is propitious for proton transfer.

The decrease by a factor of ∼4 of the diffusional rate constant k_q^3 of quenching of the 44BPY T_1 state by electron transfer upon addition of up to 15 % water to acetonitrile (Figure 5) follows also approximately the evolution of the preferential solvation of 44BPY by water (as reflected by the frequency variation shown in Figure 1). This decrease corresponds thus to the transition from the electron-transfer reaction regime leading to the CIP (Scheme 3) to that producing the HIP (Scheme 4). In the hypothesis that the HIP corresponds to a SSIP, the observed k_q^3 decrease may be due, to some extent, to the increase of the electron acceptor to donor distance when 44BPY is H-bonded to water. It may also result from the fact that hydrogen bonding to the amine is expected to reduce its electron donor character by increasing the activation energy for the reaction, because the hydrogen bond must be broken prior to transfer.[35] However, in these interpretations, the notable increase of k_q^3 in the water-rich region, on going from 80% to 100% water (see Figure 5), remains unexplained. An alternative interpretation based on the solvent mixture viscosity can account for the k_q^3 variation observed in both the acetonitrile-rich and water-rich regions. As proposed previously,[2] since the quenching reaction is a diffusional process, its rate constant must depend inversely on the solvent viscosity. The value of k_q^3 in pure water is indeed 2.5 times weaker than the value in pure acetonitrile, in agreement with the 2.6 viscosity ratio of these solvents. In the region where the two solvents are mixed, k_q^3 is roughly 2 times weaker than that obtained in pure water. This can be accounted for by the fact that the structural change resulting from the break of the infinite water network upon adding acetonitrile to water is accompanied by an increase of the global viscosity of the solvent mixture and a slowing of its dynamics.[15,22,36,37] The increase of k_q^3 in the 80−100% water range occurs in a solvent composition range where it is agreed[19,23,38,39] that inhomogeneities in the solvent mixture disappear progressively to let the infinite hydrogen bonding network restore. We conclude that the whole variation of k_q^3 in Figure 5 is mainly reflecting the change in viscosity of the solution as the solvent composition changes.

A last point to consider is the kinetics of formation of the $44BPYH^{\bullet}$ radical in the presence of water. We have shown above that, in the HIP, the intrapair proton transfer (k_{PT}) from $TEA^{+\bullet}$ to the H-bonded $44BPY^{-\bullet}$ species does not occur but, instead, proton transfer from water takes place with a rate constant (k_H) dependent on the third power of the water concentration in the 10−100% water range (Figure 6). Therefore, although the proton transfer is likely occurring within the hydrogen-bonded $44BPY^{-\bullet}\cdots HO-H$ complex, the reaction does not correspond to a conventional intracomplex transfer, in which case a constant k_H value should have been observed over the whole range of existence of the HIP, that is, according to the preferential solvation effect, in the ∼10% to 100% water concentration domain. It does not correspond either to a simple diffusional (pseudo-first-order) quenching process between a donor and an acceptor. The remarkable dependence of k_H on a power ∼3 of water concentration indicates that roughly three water molecules are required in the vicinity of $44BPY^{-\bullet}$ for the intracomplex proton transfer to take place. It suggests that the intracomplex proton transfer is governed by the dynamics of solvation of the residual OH^- and that this solvation process requires three water molecules, according to eq 2

$$(44BPY^{-\bullet}\cdots HO-H) + 3H_2O \rightarrow 44BPYH^{\bullet} + [OH^-(H_2O)_3] \quad (2)$$

Note that the reaction can be a one-step process, as in eq 2, or a two-step process, in which case the proton jump occurs first and is followed by back transfer if the released hydroxide is not rapidly solvated by a three-water entity. Similar nonlinearity in the proton-transfer rate constant has been observed in the case of proton donation from photoacids to water in a variety of aqueous two-component-solvent mixtures.[40−45] Robinson and collaborators attributed this unusual behavior to the fact that the reaction is controlled by the hydration of the released proton, which requires a specific water structure.[41−45] They inferred that the proton acceptor is a cluster composed of a minimum of four water molecules (eq 3).

$$AH + 4H_2O \rightarrow A^- + [H_3O^+(H_2O)_3] \quad (3)$$

In pure water, the reaction is controlled by rotational fluctuations of water molecules into appropriate orientations to accept the charge. In mixed solutions, the nonlinearity with increasing concentration of the nonaqueous solvent is due to the breaking of the water clusters and the appearance of a complex diffusional regime, the reaction rate being limited by the time required to buildup a local concentration of four water molecules.[43] A comparable nonlinear dependence on water concentration has been observed for the proton abstraction process by the photoexcited 6-methoxyquinoline and explained similarly by the need for a four-water cluster in the vicinity of the basic solute B to release a proton and solvate the residual OH^- species (eq 4)[46]

$$B + 4H_2O \rightarrow BH^+ + [OH^-(H_2O)_3] \quad (4)$$

Giving the fact that, in eq 2, one water molecule is already H-bonded to the $44BPY^{-\bullet}$ base, eq 2 and eq 4 are strictly equivalent. The concept of proton and hydroxide ion hydration by small water clusters has been firmly supported by quantum-chemical calculations.[47−52] Although a 4-fold-coordinate complex $OH^-(H_2O)_4$ has been first predicted from ab initio molecular dynamics studies of the hydration of OH^-,[48,49] more recent theoretical simulations[51,52] together with spectroscopic[53] and thermochemical[54] measurements converge on the common view that $OH^-(H_2O)_3$ is the dominating coordination structure for OH^- in water. This trihydrated structure is in excellent agreement with the assumption in eq 2 that a diffusional process of kinetic order parameter equal to 3, corresponding to the solvation of OH^-, is the rate-limiting step in the intracomplex protonation of $44BPY^{-\bullet}$ by water.

However, the fact that the linear character of the logarithmic plot of k_H (Figure 6) extents from 10% to 100% water, suggesting a diffusion-controlled process on this whole range of solvent composition, remains puzzling. It is hard to understand, in regard to the claimed microheterogeneous structure of the acetonitrile−water mixtures,[13−22] how a diffusional regime can be preserved in the water-rich region. In fact, in

this region, the 44BPY$^{-\bullet}$···HO−H complex is expected to be preferentially solvated in large aqueous microdomains, with the H-bonded water molecule itself connected through H-bonds to other water molecules present in the vicinity. Thus the solvation of OH^- by a three-water entity should be essentially static at high water concentration and should not obey a kinetic law in $[H_2O]^3$. Two tentative explanations can be suggested to try to account for the contradiction between this expectation and the experiment. First, the microheterogeneous structure of the acetonitrile−water mixture could be destroyed in our experimental conditions, for example due to the presence of high concentrations (>0.1 M) of the electron donor amine (TEA or DABCO), preserving a diffusional regime for the OH^- hydration at all solvent compositions. An alternative explanation could be that the 44BPY$^{-\bullet}$···HO−H complex is actually preferentially solvated in aqueous microdomains but the static process of OH^- solvation by surrounding water molecules would be strongly influenced by the decrease in size of these domains as the acetonitrile concentration increases: the smaller the aqueous domain, the higher the activation barrier for OH^- solvation and the slower the intracomplex proton transfer. This presupposes that there is a crucial influence of the structure and dynamics of the entire microdomain water network on the reaction rate, which is consistent with the prediction by several authors that, in water, proton transfer is strongly controlled by structure fluctuation in the hydrogen bond network.[48,55−58] The time scale of these collective molecular motions associated with the hydrogen bond network rearrangement was found to be ≤10 ps. It is consistent with the fast protonation time constant ($1/k_H$ = 13 ps) measured for 44BPY$^{-\bullet}$ in pure water. Upon addition of acetonitrile, the water structure is broken and aqueous microdomains appear, resulting in a slowing of the solvent dynamics.[15,22,36,37] The concomitant decrease of k_H indicates an increasing difficulty for the hydrogen-bond network fluctuation to allow water molecules in the 44BPY$^{-\bullet}$ solvent shell to adopt a cluster configuration appropriate to OH^- hydration as the size of this microdomain decreases. Recent investigations of excited-state proton transfer in solvent clusters have underlined the importance of solvent structure and cluster size on the reaction rate.[59,60] For instance, upon excitation, 1-naphthol undergoes proton transfer to water on a nanosecond time scale for a cluster of several hundred water molecules[61] whereas the reaction occurs in 32 ps in bulk water.[43] However, even if, on going from the acetonitrile-rich region to the water-rich region, the hydroxyl solvation process changes from a diffusional regime to a static regime strongly influenced by the size of the water microdomain, it is hard to explain why the dependence of the rate constant k_H on the third power of the water content is maintained unchanged. This dependence remains not convincingly explained and a more accurate investigation of the k_H variation in the water-rich region (the plot of Figure 6 comprises only two measurements in this region) appears necessary to get a more reliable understanding of the complex influence of the solvent structural and dynamical properties on the proton-transfer dynamics in aqueous solution.

Another experimental indication of the crucial influence of the H-bond network structure and dynamics on the intracomplex proton-transfer rate is the observed dependence of k_H on the DABCO concentration in the acetonitrile/water mixtures (Figure 8). An inverse relationship is found between k_H and the basicity of the water bath. The same trend was observed previously in pure aqueous solution on intensifying the basicity by increasing the DABCO concentration or adding KOH.[2] This effect can be explained by the fact that in the presence of a fairly concentrated basic solute, here DABCO or KOH, the water network must adopt a structural configuration favoring the solvation of this solute by H-bonding. Increasing the DABCO (KOH) concentration reinforces this solvent organization, the H-bond network being more and more strongly oriented toward the amine electron pairs. As a consequence, the solvent reorganization necessary to drive the proton transfer within the 44BPY$^{-\bullet}$···HO−H complex, i.e., generate the cluster configuration appropriate to the accommodation of the residual OH^- species by hydration, becomes more and more energetic. This increasing barrier to solvent reorientation can be assumed to account to a certain extent for the decrease of the intracomplex proton-transfer rate constant k_H observed in Figure 8. However, it must be kept in mind that, given the high concentrations in DABCO used in these measurements (0.1−0.8 M), the volume occupied in the solution by this donor species itself is likely interfering with the ability of three water molecules to solvate the hydroxide. This steric effect must also contribute to the decrease of k_H observed upon increasing the DABCO concentration in such a way that the role of DABCO/water interactions discussed above must be tempered.

Conclusion

The photoreduction of 44BPY by DABCO and TEA in acetonitrile−water mixtures has been investigated by using picosecond transient absorption and time-resolved resonance Raman spectroscopy. First, the state of solvation of the 44BPY solute in the ground state was probed by analyzing the Raman spectrum as a function of the solvent mixture composition. It turns out that 44BPY is hydrogen bonded to water molecules as soon as water reaches a concentration of 10% in volume, which is indicative of a preferential solvation of the heterocyclic solute in aqueous microdomains.

Below 10% water, the photoreduction of the free 44BPY leads to a contact ion pair (44BPY$^{-\cdot}$, amine$^{+\cdot}$) (CIP) that undergoes, as in neat acetonitrile, efficient intrapair proton transfer if TEA is the amine donor. Above 10% water, the photoreduction of the H-bonded 44BPY leads to a hydrated ion pair (44BPY$^{-\bullet}$··· HO−H, amine$^{+\bullet}$), in which the intrapair proton transfer is inhibited. Instead, the 44BPY$^{-\bullet}$ species is protonated by water through the hydrogen bond, resulting in a pOH jump in the solution. The rate constant k_H for this intracomplex proton transfer process depends strongly on the solvent composition, increasing roughly as the third power of the water concentration from 10 to 100% water. We interpret this result by assuming that the intracomplex proton transfer is controlled by the stabilization of the residual OH^- species by hydration within a three-water cluster $OH^-(H_2O)_3$. However it is quite surprising to observe this diffusional regime even in the water-rich region where the presence of large aqueous microdomains is expected to favor a static regime for the OH^- solvation. This inconsistency remains to be explained, and a more careful examination of the reaction dynamics in the water-rich region is planned for this purpose.

Acknowledgment. The authors thank the Groupement de Recherche GDR 1017 from CNRS and the Centre d'études et de Recherches Lasers et Applications (CERLA) for their help in the development of this work. CERLA is supported by the Ministère chargé de la Recherche, Région Nord/Pas de Calais, and the Fonds Européen de Développement Economique des Régions.

References and Notes

(1) Boilet, L.; Burdzinski, G.; Buntinx, G.; Lefumeux, C.; Poizat, O. *J. Phys. Chem. A* **2001**, *105*, 10271.

(2) Boilet, L.; Buntinx, G.; Lefumeux, C.; Poizat, O. *J. Phys. Chem. A* **2002**, *106*, 10222.
(3) Herodes, K.; Leito, I.; Koppel, I.; Rosés, M. *J. Phys. Org. Chem.* **1999**, *12*, 109.
(4) Leitao, R. E.; Martins, F.; Ventura, M. C.; Nunes, N. *J. Phys. Org. Chem.* **2002**, *15*, 623.
(5) Buntinx, G.; Naskrecki, R.; Poizat, O. *J. Phys. Chem.* **1996**, *100*, 19380.
(6) Didierjean, C.; Dewaele, V.; Buntinx, G.; Poizat, O. *Chem. Phys.* **1998**, *237*, 169.
(7) Didierjean, C.; Buntinx, G.; Poizat, O. *J. Phys. Chem. A* **1998**, *102*, 7938.
(8) Bertie, J. E.; Lan, Z. *J. Phys. Chem. B* **1997**, *101*, 4111.
(9) Takamuku, T.; Tabata, M.; Yamaguchi, A.; Nishimoto, J.; Kumamoto, M.; Wakita, H.; Yamaguchi, T. *J. Phys. Chem. B* **1998**, *102*, 8880.
(10) Venables, D. S.; Schmuttenmaer, C. A. *J. Chem. Phys.* **1998**, *108*, 4935.
(11) Nishikawa, K.; Kasahara, Y.; Ichioka, T. *J. Phys. Chem. B* **2002**, *106*, 693.
(12) Tee, E. M.; Awichi, A.; Zhao, W. *J. Phys. Chem. A* **2002**, *106*, 6714.
(13) Jamroz, D.; Stangret, J.; Lindgren, J. *J. Am. Chem. Soc.* **1993**, *115*, 6165.
(14) Bergman, D. L.; Laaksonen, A. *Phys. Rev. E* **1998**, *58*, 4706.
(15) Mountain, R. D. *J. Phys. Chem. A* **1999**, *103*, 10744.
(16) Mountain, R. D. *Int. J. Thermophys.* **2001**, *1*, 101.
(17) Venables, D. S.; Schmuttenmaer, C. A. *J. Chem. Phys.* **2000**, *113*, 11222.
(18) Reimers, J. R.; Hall, L. E. *J. Am. Chem. Soc.* **1999**, *121*, 3730.
(19) Reichardt, C. *Solvents and Solvent Effects in Organic Chemistry*, 2nd ed.; VCH: Weinheim, 1988.
(20) Reichardt, C. *Chem. Rev.* **1994**, *94*, 2319.
(21) Herodes, K.; Leito, I.; Koppel, I.; Rosés, M. *J. Phys. Org. Chem.* **1999**, *12*, 109.
(22) Krolicki, R.; Jarzeba, W.; Mostafavi, M.; Lampre, I. *J. Phys. Chem. A* **2002**, *106*, 1708.
(23) Molotsky, T.; Huppert, D. *J. Phys. Chem. A* **2003**, *107*, 2769.
(24) Kihara, H.; Gondo, Y. *J. Raman Spectrosc.* **1986**, *17*, 263.
(25) Elisei, F.; Mazzucato, U.; Görner, H.; Schulte-Frohlinde, D *J. Photochem. Photobiol., A* **1989**, *50*, 209.
(26) Poizat, O.; Buntinx, G.; Valat, P.; Wintgens, V.; Bridoux, M. *J. Phys. Chem.* **1993**, *97*, 5905.
(27) Buntinx, G.; Valat, P.; Wintgens, V.; Poizat, O. *J. Phys. Chem.* **1991**, *95*, 9347.
(28) Poizat, O.; Buntinx, G.; Ventura, M.; Lautié, M. F. *J. Phys. Chem.* **1991**, *95*, 1245.
(29) Ould-Moussa, L.; Poizat, O.; Castella-Ventura, M.; Buntinx, G.; Kassab, E. *J. Phys. Chem.* **1996**, *100*, 2072.
(30) Griller, S.; Howard, J. A.; Marriott, P. R.; Scaiano, J. C. *J. Am. Chem. Soc.* **1981**, *103*, 619.
(31) Borgis, D. C.; Lee, S.; Hynes, J. T. *Chem. Phys. Lett.* **1989**, *162*, 19.
(32) Borgis, D. C.; Lee, S.; Hynes, J. T. *J. Chem. Phys.* **1991**, *94*, 3619.
(33) Borgis, D. C.; Lee, S.; Hynes, J. T. *J. Phys. Chem.* **1996**, *100*, 1118.
(34) Peters, K. S.; Cashin, A.; Timbers, P. *J. Am. Chem. Soc.* **2000**, *122*, 107.
(35) Simon, J. D.; Peters, K. S. *J. Am. Chem. Soc.* **1982**, *104*, 6542.
(36) Goldammer, E. V.; Hertz, H. G. *J. Phys. Chem.* **1970**, *74*, 3734.
(37) Kovacs, H.; Laaksonen, A. *J. Am. Chem. Soc.* **1991**, *113*, 5596.
(38) Moreau, C.; Douheret, G. *J. Chem. Thermodyn.* **1976**, *8*, 403.
(39) Douheret, G.; Moreau, C.; Viallard, A. *Fluid Phase Equilib.* **1985**, *22*, 289.
(40) Huppert, D.; Kolodney, G. *Chem. Phys.* **1981**, *63*, 401.
(41) Lee, J.; Griffine, R. D.; Robinson, G. W. *J. Chem. Phys.* **1985**, *82*, 4920.
(42) Robinson, G. W.; Thistlethwaite, P. J.; Lee, J. *J. Phys. Chem.* **1986**, *90*, 4224.
(43) Lee, J.; Robinson, G. W.; Webb, S. P.; Philips, L. A.; Clark, J. H. *J. Am. Chem. Soc.* **1986**, *108*, 6538.
(44) Lee, J. *J. Am. Chem. Soc.* **1989**, *111*, 427.
(45) Fillingim, T. G.; Luo, N.; Lee, J.; Robinson, G. W. *J. Phys. Chem.* **1990**, *94*, 6368.
(46) Yao, S. H.; Lee, J.; Robinson, G. W. *J. Am. Chem. Soc.* **1990**, *112*, 5698.
(47) Eigen, M. *Angew. Chem., Int. Ed.* **1964**, *3*, 1.
(48) Marx, D.; Tuckerman, M. E.; Hutter, J.; Parrinello, M. *Nature* **1999**, *397*, 601.
(49) Tuckerman, M. E.; Marx, D.; Parrinello, M. *Nature* **2002**, *417*, 925.
(50) Nova, J. J.; Mota, F.; delValle, C. P.; Plans, M. *J. Phys. Chem. A* **1997**, *101*, 7842.
(51) Asthagiri, D.; Pratt, L. R.; Kress, J. D.; Gomez, M. A. *Chem. Phys. Lett.* **2003**, *380*, 530.
(52) Asthagiri, D.; Pratt, L. R.; Kress, J. D.; Gomez, M. A. *Proc. Natl. Acad. Sci. U.S.A.* **2004**, *101*, 7229.
(53) Robertson, W. H.; Diken, E. G.; Price, E. A.; Shin, J. W.; Johnson, M. A. *Science* **2003**, *299*, 1367.
(54) Moet-Ner, M.; Speller C. V. *J. Phys. Chem.* **1986**, *90*, 6616.
(55) Kobayashi, C.; Iwahashi, K.; Saito, S.; Ohmine, L. *J. Chem. Phys.* **1996**, *105*, 6358.
(56) Ohmine, L.; Saito, S. *Acc. Chem. Res.* **1999**, *32*, 741.
(57) Steib, A.; Borgis, A.; Hynes, J. T. *J. Chem. Phys.* **1995**, *102*, 2487.
(58) Ando, K.; Hynes, J. T. *J. Phys. Chem. B* **1997**, *101*, 10464.
(59) Syage, J. A. *J. Phys. Chem.* **1995**, *99*, 5772.
(60) Zhong, Q.; Castleman, A. V. *Chem. Rev.* **2000**, *100*, 4049.
(61) Knochenmuss, R.; Holtom, G. R.; Ray, D. *Chem. Phys. Lett.* **1993**, *215*, 188.